J. Phys. B: At. Mol. Opt. Phys. 25 (1992) L605-L612. Printed in the UK

LETTER TO THE EDITOR

The contributions of double excitation–autoionization to the electron impact ionization of Li^+

D C Griffin†, M S Pindzola‡ and N R Badnell‡

† Department of Physics, Rollins College, Winter Park, FL 32789, USA
‡ Department of Physics, Auburn University, Auburn, AL 36849, USA

Received 24 August 1992

Abstract. We have performed 11-state and 37-state *R*-matrix close-coupling calculations of the contributions of double excitation followed by autoionization to the electron impact ionization cross section of Li^+. Through the use of pseudo-orbitals in the configuration-interaction expansions for the bound states, we obtained energies in good agreement with observed energies for both the singly excited and doubly excited terms. The 37-state calculation, which employed a basis set with a total of 58 terms in all of the configuration-interaction expansions, is an improvement over our earlier calculation of this process and predicts a resonance structure which is in general agreement with that observed in an earlier high-resolution measurement of this process.

In an earlier paper (Pindzola and Griffin 1990), we considered the contributions to the ionization cross section of Li^+ from double excitation followed by single autoionization and double excitation with capture followed by simultaneous double autoionization, and we compared our calculated results with high-resolution measurements of these indirect contributions (Müller *et al* 1989). In order to treat the first of these two complex processes, we performed an 11-state close-coupling calculation which included terms arising from singly excited configurations of the form $1s2l$ and doubly excited configurations of the form $2l2l'$ using the program IMPACT (Crees *et al* 1978). Since the branching ratios for autoionization from terms of the configurations $2l2l'$ are nearly equal to unity, the total cross section for transitions of the type $1s^2 \rightarrow 2l2l'$ is equal to that of double excitation-autoionization. However, there were some basic problems associated with this earlier calculation.

First of all, two-electron transitions to the doubly excited states $2l2l'$ occur primarily through coupling with singly excited configurations of the form $1s2l$. Furthermore, in a close-coupling calculation, one must use a unique set of orbitals to represent all states included in the close-coupling expansion. But a complication arises from the fact that the $2l$ orbitals in the singly excited configurations $1s2l$ are well shielded by the 1s orbital and, therefore, occur at a larger radius than the $2l$ orbitals in the doubly excited configurations. Thus a calculation which employed $2l$ orbitals determined from Hartree-Fock (HF) calculations for the doubly excited states would yield artificially large cross sections to the singly excited states and, through continuum coupling, to the doubly excited states. As a compromise in our earlier calculation, we employed $2l$ orbitals determined from HF calculations for the singly excited states and then adjusted the energies of the doubly excited states used in the close-coupling calculation to the energies obtained from a HF calculation for the doubly excited states. However, as we

0953-4075/92/230605+08$07.50

shall see, a much more consistent method for treating the difference between the $2l$ orbitals in the singly and doubly excited configurations is possible through the use of pseudo-orbitals.

In addition, the 11-state calculation did not include doubly excited states of the form $2l3l'$. Yet transitions to these states will contribute to the double excitation cross section in the energy range of the experimental measurements and recombination resonances of the form $2l3l'nl''$ can contribute to the cross section to states of the configurations $2l2l'$.

Our first step in repeating the analysis of these double electron excitation transitions was to carry out another 11-state calculation. However, this time we employed the basis set described in table 1, which was generated using Fischer's multiconfiguration Hartree–Fock (MCHF) code (Fischer 1991). The 2s and 2p orbitals were determined from single configuration HF calculations for the doubly excited states. Then the $3\bar{s}$ and $3\bar{p}$ pseudo-orbitals were generated from MCHF calculations in which the $2l$ orbitals were frozen and the $3l$ orbitals allowed to relax to correct the 2s and 2p orbitals for the difference between a $2l$ orbital in $2l^2$ and $1s2l$. The multiconfiguration radial wavefunctions determined in this way are identical to those obtained from a single-configuration HF calculation for the singly excited configurations $1s2l$. These orbitals were then used to generate the configuration-interaction expansions involving the terms listed in table 1. The 11 terms in this list which did not involve pseudo-orbitals were included in the close-coupling expansion and their energies are shown in table 2, in comparison with experiment.

Table 1. Basis set #1 employed for the 11-state calculation.

Three of the five orbitals employed in this calculation were determined from single-configuration HF calculations as follows: 1s from $1s^2\,{}^1S$, 2s from $2s^2\,{}^1S$, and 2p from $2p^2\,{}^1S$. The $3\bar{s}$ pseudo-orbital was generated from a MCHF calculation on the $1s2s\,{}^1S + 1s3\bar{s}\,{}^1S$ terms and the $3\bar{p}$ pseudo-orbital was generated from a MCHF calculation on the $1s2p\,{}^1P + 1s3\bar{p}\,{}^1P$ terms.

The configuration-interaction expansions included the

nine even parity terms:

$1s^2\,{}^1S$, $1s2s\,{}^1S$, $1s3\bar{s}\,{}^1S$, $2\bar{s}^2\,{}^1S$, $2\bar{p}^2\,{}^1S$ $1s\bar{2}s\,{}^3S$, $1s3\bar{s}\,{}^3S$, $2p^2\,{}^3P$, $2p^2\,{}^1D$;

and the six odd parity terms:

$1s2p\,{}^3P$, $1s3\bar{p}\,{}^3P$, $2s2p\,{}^3P$, $1s2p\,{}^1P$, $1s3\bar{p}\,{}^1P$, $2s2p\,{}^1P$.

We have employed the R-matrix method as coded for the Opacity Project (Berrington *et al* 1987) to carry out the close-coupling calculations. In the scattering calculation, the excited state thresholds were adjusted to the experimental energies, where available. As is often done in close-coupling calculations, we included in the bound-state part of the close-coupling expansion all $(N+1)$-electron configurations which could be formed by adding each of the orbitals included in the calculation to all of the N-electron terms employed in the configuration-interaction expansions, rather than just those terms employed in the close-coupling expansion. This allows for a more complete description of correlation in the $(N+1)$-electron system. However, when the N-electron configurations involve pseudo-orbitals, this leads to the presence of

Table 2. Li^+ Energies (eV) for terms included in 11-state close-coupling calculation using basis set #1.

	Term	Theoretical energies	Experimental energies
1	$1s^2\ ^1S$	0.00	0.00
2	$1s2s\ ^3S$	59.01	59.02[a,b]
3	$1s2s\ ^1S$	60.44	60.93[b]
4	$1s2p\ ^3P$	61.04	61.28[a,b]
5	$1s2p\ ^1P$	62.07	62.22[a,b]
6	$2s^2\ ^1S$	145.30	146.26[c]
7	$2s2p\ ^3P$	146.21	147.00[c]
8	$2p^2\ ^3P$	148.43	
9	$2p^2\ ^1D$	149.86	149.94[c]
10	$2s2p\ ^1P$	150.68	150.30[c]
11	$2p^2\ ^1S$	154.25	153.75[c]

[a] Moore (1971).
[b] Bashkin and Stoner (1975).
[c] Rødbro *et al* (1979).

pseudo-resonances. We investigated these resonances and found that they did not occur close to the energy range of interest. Finally, the partial-wave expansion was found to converge with respect to the double excitation cross section by including partial waves only up to a total angular momentum of four.

In figure 1, the results of the 11-state calculation for the total cross section to the six doubly excited states listed in table 2 are shown in comparison with the crossed-beams measurements of Müller *et al* (1989). The experimental measurements are the difference between the total ionization cross section and the smooth direct ionization cross section background. The theoretical curve above 150 eV is quite similar to the result we obtained in our earlier calculation (Pindzola and Griffin 1990); this indicates that the approximate method we used formerly to handle the difference between the $2l$ orbitals in the singly and doubly excited states, without the use of pseudo-orbitals,

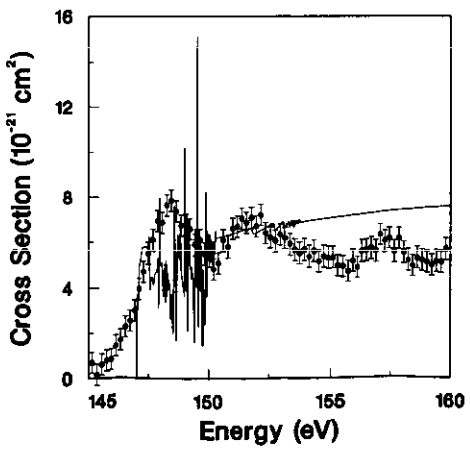

Figure 1. Total double-excitation cross section to the terms of $2l2l'$ in Li^+ from the 11-state R-matrix close-coupling calculation. The full circles are the experimental measurements of the difference between the total ionization cross section and a smooth direct ionization cross section from Müller *et al* (1989).

was reasonable. Below 150 eV, in the region of the first broad peak in the experiment, there are a series of resonances due to recombination into Rydberg states attached to higher energy $2l2l'$ terms. There was evidence for such a resonance structure in our earlier 11-state calculation, but there was not a sufficient number of energy points to determine the detailed resonance structure.

In figure 2, we show the calculated cross section, after being convoluted with a 1.2 eV Gaussian in order to simulate the experimental electron energy distribution. As can be seen, the resonance peak is now quite small compared with the experimental curve. In addition, the two broad resonance structures above 150 eV, which are observed in the experiment, are not seen in this calculation. They must be due to recombination into Rydberg states attached to higher energy doubly excited states such as $2l3l'$ that, as mentioned above in our discussion of our earlier calculation, are not included in the 11-state calculation.

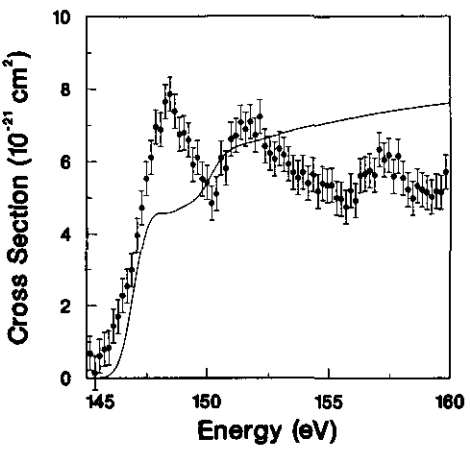

Figure 2. Same as figure 1, except the theoretical curve is convoluted with a 1.2 eV Gaussian to simulate the experimental electron energy distribution.

In order to more completely account for the structure of the experimental cross section, we performed a much larger calculation, which included all the terms of the $2l3l'$ configurations in the close-coupling expansion. Basis set #2, which was employed in this 37-state calculation is described in table 3. The 1s and $2l$ orbitals are identical to those employed in basis set #1. However, in this case, the $3l$ orbitals are spectroscopic, being determined from single-configuration HF calculations. In order to correct the 2s and 2p orbitals, and to a lesser extent the 3s and 3p orbitals, in the singly excited states for the fact that they were calculated using single-configuration HF calculations for the doubly excited states, we performed MCHF calculations to generate the $4\bar{s}$ and $4\bar{p}$ pseudo-orbitals. These MCHF calculations were performed in a way similar to that described above for basis set #1.

These orbitals were then used to construct configuration-interaction expansions employing the 58 terms listed in the second part of table 3. The energies obtained from this configuration-interaction calculation are compared with the experimental values for all terms arising from the singly excited configurations $1s^2$, $1s2l$, $1s3l$ and the doubly excited configurations $2l2l'$ and $2l3l'$ in table 4. It is these 37 terms that were included in the close-coupling expansion.

Table 3. Basis set #2 employed for the 37-state calculation.

Six of the eight orbitals included in this calculation were determined from single-configuration HF calculations as follows: 1s from $1s^2\ ^1S$, 2s from $2s^2\ ^1S$, 2p from $2p^2\ ^1S$, 3s from $2s3s\ ^1S$, 3p from $2p3p\ ^1S$, and 3d from $2p3d\ ^1P$. The $4\bar{s}$ pseudo-orbital was determined from a MCHF calculation on the $1s2s\ ^1S + 1s3s\ ^1S + 1s4\bar{s}\ ^1S$ terms. The $4\bar{p}$ pseudo-orbital was determined from a MCHF calculation on the $1s2p\ ^1P + 1s3p\ ^1P + 1s4\bar{p}\ ^1P$ terms.

The configuration interaction expansions included the

32 even parity terms:

$1s^2\ ^1S$,	$1s2s\ ^1S$,	$1s3s\ ^1S$,	$1s4\bar{s}\ ^1S$,	$2s^2\ ^1S$,	$2p^2\ ^1S$,
$2s3s\ ^1S$,	$2p3p\ ^1S$,	$3s^2\ ^1S$,	$3p^2\ ^1S$,	$3d^2\ ^1S$,	$1s2s\ ^3S$,
$1s3s\ ^3S$,	$1s4\bar{s}\ ^3S$,	$2s3s\ ^3S$,	$2p3p\ ^3S$,	$2p^2\ ^3P$,	$2p3p\ ^3P$,
$3p^2\ ^3P$,	$3d^2\ ^3P$,	$2p3p\ ^1P$,	$1s3d\ ^3D$,	$2s3d\ ^3D$,	$2p3p\ ^3D$,
$3s3d\ ^3D$,	$1s3d\ ^1D$,	$2p^2\ ^1D$,	$2s3d\ ^1D$,	$2p3p\ ^1D$,	$3s3d\ ^1D$,
$3p^2\ ^1D$,	$3d^2\ ^1D$;				

and the 26 odd parity terms:

$1s2p\ ^3P$,	$1s3p\ ^3P$,	$1s4\bar{p}\ ^3P$,	$2s2p\ ^3P$,	$2s3p\ ^3P$,	$2p3s\ ^3P$,
$2p3d\ ^3P$,	$3s3p\ ^3P$,	$3p3d\ ^3P$,	$1s2p\ ^1P$,	$1s3p\ ^1P$,	$1s4\bar{p}\ ^1P$,
$2s2p\ ^1P$,	$2s3p\ ^1P$,	$2p3s\ ^1P$,	$2p3d\ ^1P$,	$3s3p\ ^1P$,	$3p3d\ ^1P$,
$2p3d\ ^3D$,	$3p3d\ ^3D$,	$2p3d\ ^1D$,	$3p3d\ ^1D$,	$2p3d\ ^3F$,	$3p3d\ ^3F$,
$2p3d\ ^1F$	$3p3d\ ^1F$.				

The 37-state R-matrix close-coupling calculation was carried out in a way similar to that already described for the 11-state calculation. That is, the energies were adjusted to the experimental values, where available; the bound part of the close-coupling expansion included all $(N+1)$-electron terms which could be constructed from the 58 terms included in the configuration-interaction expansions; and convergence of the partial-wave expansion with respect to the double-excitation cross section was achieved by including partial waves only up to $L=4$. Even then, this was a very time consuming calculation because of the number of states included and the large size of the R-matrix boundary needed with the inclusion of the 3d, $4\bar{s}$ and $4\bar{p}$ orbitals.

The results for the double excitation cross section in comparison to experiment are shown in figure 3. We now see clear evidence of pronounced resonance structures in the regions of the three broad peaks observed in the experiment. In addition, although the resonance structure above 155 eV is large compared with the third broad peak in the experiment, the background cross section appears to be closer to the experimental measurements before the onset of these resonances.

In order to make a more meaningful comparison with the experiment, we again convoluted the calculated cross section with a 1.2 eV Gaussian and this curve is shown in figure 4. The agreement between experiment and theory at threshold is now better than in the case of the 11-state calculation. In addition, the presence of three broad peaks is visible in the calculation, and the theory even predicts the rise in the cross section just before 160 eV, which is also seen in the experimental curve. However, it is disappointing that the dip between the first and second broad peak is hardly visible and the third broad peak is lower in energy and larger than that seen in the experimental curve.

There are several possible explanations for these remaining discrepancies. First of all, the recombination resonances will only contribute to the ionization cross section

Table 4. Li^+ Energies (eV) for terms included in 37-state close-coupling calculation using basis set #2.

	Term	Theoretical energies	Experimental energies
1	$1s^2\,^1S$	0.00	0.00
2	$1s2s\,^3S$	58.91	59.02[a,b]
3	$1s2s\,^1S$	60.44	60.93[b]
4	$1s2p\,^3P$	60.99	61.28[a,b]
5	$1s2p\,^1P$	62.01	62.22[a,b]
6	$1s3s\,^3S$	68.50	68.78[a]
7	$1s3s\,^1S$	68.94	69.28[a]
8	$1s3p\,^3P$	69.11	69.37[a]
9	$1s3d\,^3D$	69.31	69.59[a]
10	$1s3d\,^1D$	69.32	69.59[a]
11	$1s3p\,^1P$	69.39	69.65[a]
12	$2s^2\,^1S$	145.30	146.26[c]
13	$2s2p\,^3P$	146.09	147.00[c]
14	$2p^2\,^3P$	148.44	
15	$2p^2\,^1D$	149.71	149.94[c]
16	$2s2p\,^1P$	150.40	150.30[c]
17	$2p^2\,^1S$	154.08	153.75[c]
18	$2s3s\,^3S$	158.52	158.98[c]
19	$2s3s\,^1S$	158.90	159.64[c]
20	$2s3p\,^1P^*$	159.04	159.20[c]
21	$2p3s\,^3P^*$	159.30	
22	$2s3d\,^3D^*$	159.76	159.92[c]
23	$2s3p\,^3P^*$	159.78	160.04[c]
24	$2p3p\,^1P$	160.16	
25	$2p3p\,^1D^*$	160.25	
26	$2p3p\,^3P$	160.39	
27	$2p3d\,^1D$	160.47	
28	$2p3d\,^3F$	160.57	160.72[c]
29	$2p3s\,^1P^*$	160.62	161.03[d]
30	$2p3d\,^3D$	160.74	161.02[c]
31	$2p3p\,^3D$	160.77	
32	$2p3p\,^3S$	160.90	
33	$2s3d\,^1D^*$	161.08	
34	$2p3d\,^1F$	161.30	161.50[c]
35	$2p3d\,^3P$	161.34	162.08[c]
36	$2p3d\,^1P$	161.76	
37	$2p3p\,^1S$	161.79	

[a] Moore (1971).
[b] Bashkin and Stoner (1975).
[c] Rødbro *et al* (1979).
[d] Carroll and Kennedy (1977).
* Mixing between 2p3s+2s3p and between 2p3p+2s3d is so large that the configuration identifications for these terms are arbitrary.

if they autoionize to one of the N-electron doubly excited states that can autoionize again, rather than to a singly excited state which is bound. The 37-state calculation includes only a limited number of singly excited states, and the inclusion of additional states of this kind might reduce the size of the resonance contribution. Furthermore, coupling of the terms arising from the $2l2l'$ and $2l3l'$ configurations to higher energy terms, such as those arising from the $3l3l'$ configurations, might reduce the double

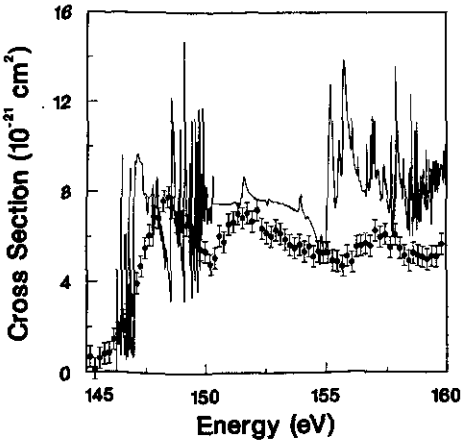

Figure 3. Total double-excitation cross section to the terms of $2l2l'$ and those of $2l3l'$ below 160 eV from the 37-state R-matrix close-coupling calculation. The full circles are the same as those described in figure 1.

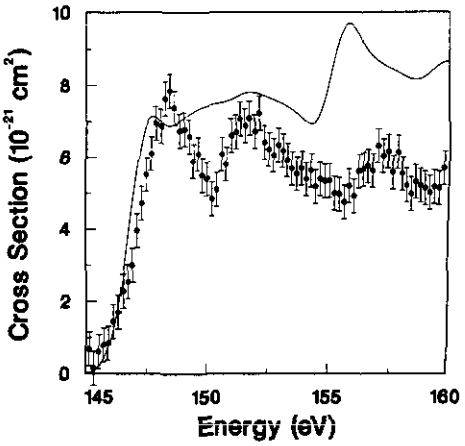

Figure 4. Same as figure 3, except the theoretical curve is convoluted with a 1.2 eV Gaussian to simulate the experimental electron energy distribution.

excitation cross section at higher energies, where the discrepancies are most pronounced. However, these additional singly and doubly excited states would make the calculation prohibitively large and time consuming.

Finally, the strength of the resonance structure is quite sensitive to the energy position of recombination resonances, since a small change in energy will determine whether a particular resonant state is open or closed for autoionization to a given N-electron term. In order to investigate this sensitivity to energy, we repeated the later stages of the 37-state calculation, without adjusting the theoretical term energies to the experimental energies. As can be seen from table 4, this energy adjustment amounted to increasing the energy of the lowest two doubly excited states by approximately one eV, while the adjustment in the higher energy thresholds was smaller, or in cases where no experimental energies were available, was non-existent. The new calculation revealed a very significant increase in both the height and width of the first set of resonances

in the threshold region. Obviously, more resonance states can autoionize to the lower two terms when the terms are at slightly lower energies.

In the light of the complexity of the double electron transitions and the uncertainties associated with even the 37-state calculation of this process, it is satisfying that the theory predicts the correct magnitude for the cross section and the general structure of the observed resonance structure.

We acknowledge C F Fischer for providing us with her latest MCHF code and for advising us on its use. We thank Tomas Brage for helping us to implement these codes and for advice on the generation of pseudo-orbitals. We want to acknowledge the members of the Opacity Project for providing us with their version of the *R*-matrix program and we thank Keith Berrington for helpful discussions on its use with respect to the inclusion of pseudo-orbitals. This work was supported by the Office of Fusion Energy, US Department of Energy under contract no DE-AC05-84OR21400 with Martin Marietta Energy Systems, Inc and contract no DE-FG05-86ER53217 with Auburn University.

References

Bashkin S and Stoner J O Jr 1975 *Atomic Energy Levels and Grotrian Diagrams* (Amsterdam: North-Holland)
Berrington K A, Burke P G, Butler K, Seaton M J, Storey P J, Taylor K T and Yan Y 1987 *J. Phys. B: At. Mol. Phys.* **20** 6379–98
Carroll P K and Kennedy E T 1977 *Phys. Rev. Lett.* **38** 1068–71
Crees M A, Seaton M J and Wilson P M H 1978 *Comput. Phys. Commun.* **15** 23–83
Fischer C F 1991 *Comput. Phys. Commun.* **64** 369–98
Moore C E 1971 *Atomic Energy Levels* NSRDS-NBS No 35 Vol 1 (Washington, DC: US Govt Printing Office)
Müller A, Hofmann G, Weissbecker B, Stenke M, Tinschert K and Salzborn E 1989 *Phys. Rev. Lett.* **63** 758–61
Pindzola M S and Griffin D C 1990 *Phys. Rev.* A **42** 6531–6
Rødbro M, Bruch P and Bisgaard P 1979 *J. Phys. B: At. Mol. Phys.* **12** 2413–47